3D ELECTROMAGNETIC MODELING USING STAGGERED FINITE DIFFERENCES

Gregory A. Newman and David L. Alumbaugh
Sandia National Laboratories
P.O. Box 5800, Albuquerque NM 87185-0750
Tel: (505) 844-8158; Fax (505) 844-7354
Email: ganewma@sandia.gov

ABSTRACT

The method of finite differences has been employed to solve a variety of 3D electromagnetic (EM) forward problems arising in geophysical applications. Specific sources considered include dipolar and magnetotelluric (MT) field excitation in the frequency domain. In the forward problem, the EM fields are simulated using a vector Helmholtz equation for the electric field, which are approximated using finite differences on a staggered grid. To obtain the fields, a complex-symmetric matrix system of equations is assembled and iteratively solved using the quasi-minimum method (QMR) method. Perfectly matched layer (PML) absorbing boundary conditions are included in the solution and are necessary to accurately simulate fields in propagation regime (frequencies > 10 MHz). For frequencies approaching the static limit (< 10 KHz), the solution also includes a static-divergence correction, which is necessary to accurately simulate MT source fields and can be used to accelerate convergence for the dipolar source problem.

INTRODUCTION

For too long the interpretation of frequency-domain electromagnetic data arising from complex geologic media has been limited by the lack of interpretation tools. It is only within the last few years that the ability to model and invert complex 3D EM data is emerging. A key reason for this development has been the application of efficient finite-difference methods to the forward modeling problem.

Over the last five years, we have developed solutions to the 3D EM forward problem for frequency-domain applications ([1] and [2]). Progress has proceeded on several fronts, including the development of a fast 3D finite difference modeling code for both dipolar and MT or natural source (plane wave) fields. Key features of the forward modeling code is its ability to simulate fields from the propagation to diffusion regime (radar to inductive EM), the inclusion of the perfectly matched layer absorbing boundary conditions necessary to reduce the size of the model domain and accurately simulate wave propagation, and the ability to model 3D variations in electrical conductivity, dielectric permittivity and magnetic permeability. The modeling code also includes a static-divergence correction, which is necessary to insure accurate MT results. In this talk, we will review our efforts in forward modeling.

THE FORWARD PROBLEM

Theory

Assuming a time harmonic dependence of $e^{i\omega t}$ where $i=\sqrt{-1}$, the vector Helmholtz equation for the electric field given by [1] is written here as

$$\nabla_e \times \mu_o/\mu\nabla_e xE + \omega\mu_o(\sigma + i\omega\varepsilon)E=S \qquad (1)$$

In this expression the electrical conductivity, magnetic permeability and dielectric permittivity are denoted by σ, μ and ε respectively, where μ_o is the magnetic permeability of free space. Specification of the source vector S, which includes the appropriate boundary conditions, determines whether dipolar or natural source (MT) field excitation is to be simulated. For dipolar source fields we have, for a total-field formulation

$$S = -i\omega\mu_o \mathbf{J_p} - i\omega \nabla_h \times (\mu_o/\mu \, \mathbf{M_p}), \qquad (2)$$

where $\mathbf{J_p}$ and $\mathbf{M_p}$ are current densities for the impressed electric and magnetic dipole sources, and Dirichlet boundary conditions are assumed with the tangential electric fields set to zero on the model domain boundary. Sometimes a scattered field formulation is desired because of accuracy considerations [2]. In this case we have

$$S=-i\omega\mu_o[(\sigma-\sigma_p) + i\omega \, (\varepsilon-\varepsilon_p)]E_p-i\omega\mu_o\nabla_h x[(\mu-\mu_o)/\mu H_p], \qquad (3)$$

where p designates background or primary values which are easy and fast to compute, such as a whole space. With a scattered field formulation the electric field, $\mathbf{E}$, in equation (1) is replaced by a scattered electric field, $\mathbf{E_s}$, where we impose the boundary condition that tangential $\mathbf{E_s}$ be zero on the boundary of the model domain. The total electric field is then given by the expression $\mathbf{E_t} = \mathbf{E_p} + \mathbf{E_s}$. In order to simulate natural source fields, S is set to zero everywhere, except at points where tangential

DISCLAIMER

DISCLAIMER

**Portions of this document may be illegible
in electronic image products. Images are
produced from the best available original
document.**

electric-field boundary values are specified. These boundary values arise from vertically propagating plane waves in layered or 2D geologic media assigned at the boundaries of the 3D problem.

The modified differential operators in equation (1) are defined by

$$\nabla_e = \mathbf{i}\ 1/e_x\ \partial/\partial_x + \mathbf{j}\ 1/e_y\ \partial/\partial_y + \mathbf{k}\ 1/e_z\ \partial/\partial_z$$

and   (4)

$$\nabla_h = \mathbf{i}\ 1/h_x\ \partial/\partial_x + \mathbf{j}\ 1/h_y\ \partial/\partial_y + \mathbf{k}\ 1/h_z\partial/\partial_z,$$

where e_j and h_j for $j = x,y,z$ are complex coordinate stretching variables which stretch the x ,y and z coordinates and define the PML absorbing boundary conditions originally developed by [5], but are in a form developed by [6] for ease of implementation.

When equation (1) is approximated with finite differences using the staggered grid due to [7], a linear system results in which the matrix is complex symmetric. This system can be efficiently solved iteratively using Krylov sub-space methods, including the quasi minimum residual (qmr) method. The reader is referred to [1] and [2] for the details on how these solvers are implemented. Once the electric fields are determined, the magnetic fields can be determined from Faraday's law, by numerically approximating the curl of the electric field at various nodal points and interpolating either the electric or magnetic field nodal values to the point of interest.

Even with the benefits of a staggered grid, which implicitly enforces the auxiliary divergence conditions on the current density,

$$\nabla_h \cdot \{(\sigma + i\omega\varepsilon)\ \mathbf{E}\} = \nabla_h \cdot \mathbf{S}/\ i\omega\mu_o, \qquad (5)$$

it is often necessary to explicitly enforce this condition through a static-divergence correction at frequencies approaching the static limit. The correction adds a term to the electric field such that equation (5) is identically satisfied and is alternated with a series of qmr iterations on equation (1). All the details on how to implement this correction procedure for either scattered and total fields can be found in [8], [9] and [10].

MT Simulations

In Figure 1, we demonstrate the 3D code's capability to simulate magnetotelluric fields which are useful in crustal investigations of the earth. The top part of the figure shows a conductive block, 2 km thick, residing in an earth with three layers. The 3D results are plotted at 1 Hz in terms of apparent resistivity and phase, given by the following formula

$$\rho^{TE} = |\ E_y/H_x\ |^2/\omega\mu_o \qquad (6)$$

$$\rho^{TM} = |\ E_x/H_y\ |^2\ /\omega\mu_o \qquad (7)$$

and

$$\theta^{TE} = \tan^{-1}\ [\mathrm{Im}(E_y/H_x\ )/\mathrm{Re}(E_y/H_x)\ ] \qquad (8)$$

$$\theta^{TM} = \tan^{-1}\ [\mathrm{Im}(E_x/H_y\ )/\mathrm{Re}(E_x/H_y)]. \qquad (9)$$

The notation TE and TM stand for transverse electric and magnetic and denote responses produced by inducing electric and magnetic fields perpendicular to the strike direction of the model. For a half-space model, the apparent resistivity will equal that of the half space, while the phase will be 45 degrees. To verify the results, we have compared the 3D responses with two 2D codes; one based on finite elements [11] and the other on finite differences that we recently developed. In the 2D case the block model is assumed to possess infinite strike length, while in the 3D case it is 80 km. Comparisons between the different codes are quite good. It must be noted that to obtain accurate 3D results a static divergence correction, as discussed above, was required for this simulation.
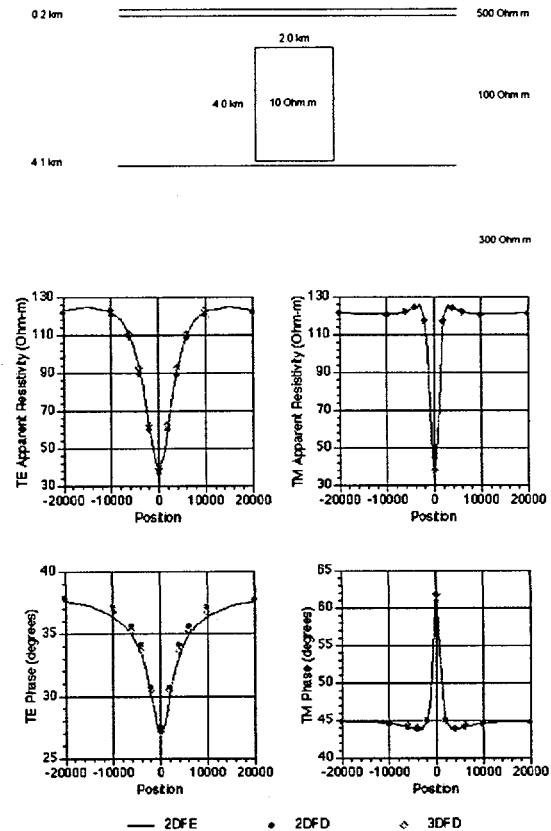

Figure 1. Comparison between 3D and 2D codes for a MT simulation at 1 Hz at the earth's surface.

The Need for PML Boundary Conditions

[1] has shown the need of the PML absorbing boundary conditions when simulating propagating fields in the frequency domain. To summarize the results, the complex stretching parameters are assigned a value of $1 + a - i b$. On the internal portions of the mesh, $a = b = 0$ such that the modified Helmholtz equation reduces to the normal form. Near edges of the mesh e_i and h_i are allowed to vary over several cells, but only in the direction that is perpendicular to the boundary. For example, along the $+z$ boundary $e_x = e_y = h_x = h_y = 1$ and only $e_z = h_z$ are allowed values of a and b that differ from zero. Some guidelines for selecting the PML stretching coordinates can be found in [1].

Figure 2 shows a simulation where the horizontal and vertical magnetic field arising from a vertical magnetic dipole and calculated on a 120 x 120 x 120 mesh for the three layer model is indicated in panel a). Resistivities of the layers are 1373, 76, 1000 Ω.m and 6, 41 and 1 are their dielectric properties relative to free space. The thickness of each layer is 1.1 and 0.9 meters. The 3D results and have been plotted against the 1D solution based on Sommerfield integrals. It is immediately evident in panel b) that the 3D solution without the PML boundary condition begins to break down at about 15 MHz, and we can assume that this is due to reflections due to the mesh boundaries contaminating the solution. Doubling the size of the cells along the mesh boundaries, that is using real grid stretching, does not help matters. Panel c) shows that poor results occur when a real stretching parameter $a = 1.0$ is employed along 25 cells of each boundary. However, when complex grid stretching is employed the results are much better. Panel d) shows results that when a stretching parameter of $b = -0.6$ is employed along 25 cells of each boundary, the fields calculated with the 3D solution match those of the 1D solution almost exactly. In panel e) we demonstrate how absorbing boundaries can be applied to shrink the size of the mesh. In this case a 72 X 72 X 72 mesh was used along with $b = -2.0$ applied for 10 cells along each boundary. Notice that both the 3D and 1D calculations coincide. This example fully illustrates the utility of the PML boundary conditions as they not only allow one to accurately simulate wave propagation, but also allow the mesh size to be significantly reduced and results in much smaller run times.
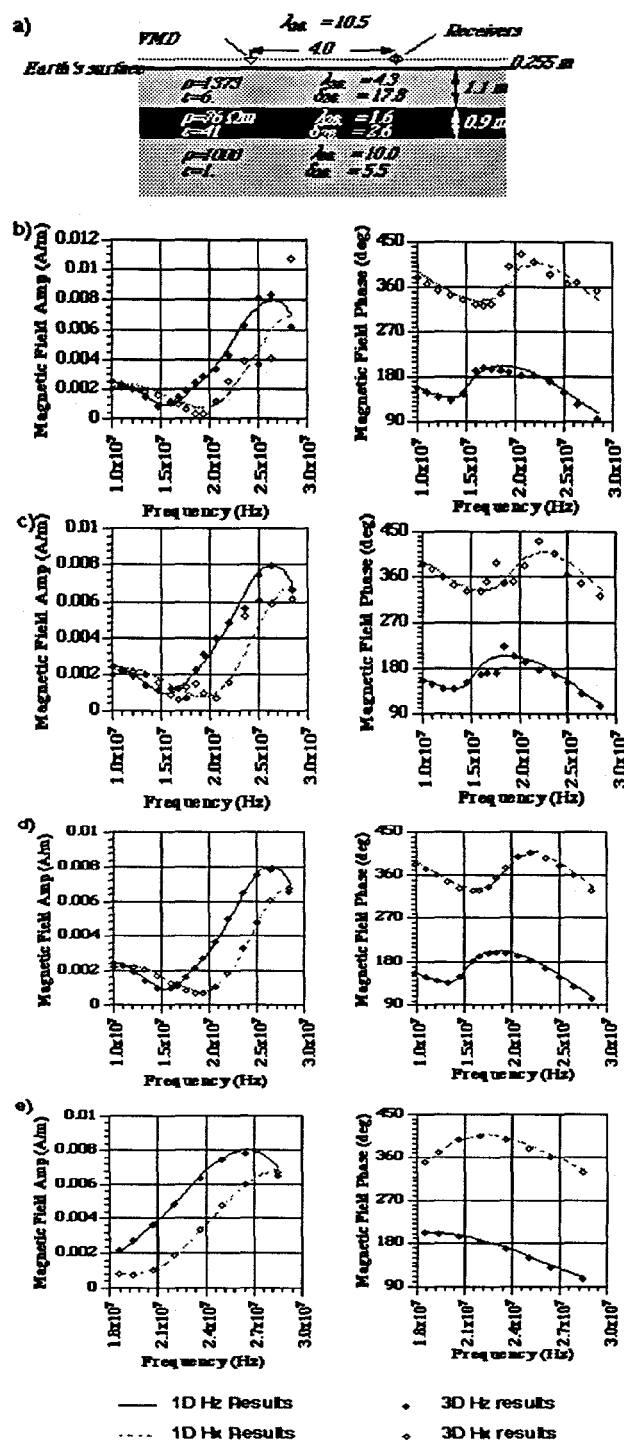
Figure 2. 1D model used to verify the need for PML absorbing boundary conditions. Note that the magnetic permeability has been set to that of free space. At the top of the figure we also have included wavelengths and skin depths in the respective layers. See text for panel explanation.

REFERENCES

[1] Alumbaugh D. L., Newman G. A., Prevost L., and Shadid, J. N., 1996, Three-dimensional wideband electromagnetic modeling on massively parallel computers: Radio Science, 31, 1-23.

[2] Newman G. A., and Alumbaugh D. L., 1995, Frequency-domain modeling of airborne electromagnetic responses using staggered finite differences: Geophysical Prospecting, 43, 1021-1042.

[3] Newman G. A., and Alumbaugh D. L., 1997, Three-dimensional massively parallel electromagnetic inversion - I. Theory: Geophysical Journal International, 128, 345-354.

[4] Alumbaugh D. L., and Newman G. A., 1997, Three-dimensional electromagnetic inversion - II. Analysis of a crosswell electromagnetic experiment: Geophysical Journal International, 128, 355-363.

[5] Berrenger J., 1993, A perfectly matched layer for the absorption of electromagnetic waves: Journal of Computational Physics, 114, 185-200.

[6] Chew W. C., and Weedon W. H., 1994, A 3D perfectly matched medium from modified Maxwell's equations with stretched coordinates: Microwave Optical Technology Letters, 7, 599-604.

[7] Yee K. S., 1966, Numerical solution of initial boundary problems involving Maxwell's equations in isotropic media: IEEE Transactions on Antennas and Propagation, AP-14, 302-309.

[8] Newman G. A., and Alumbaugh, D. L., 1996, Electromagnetic modeling of subsurface 3D structures: Presented at the International Geoscience and Remote Sensing Symposium (IGARSS), Omaha, Nebraska.

[9]Alumbaugh D. L., and Newman G. A., 1996, Electromagnetic modeling of perfect conductors in an arbitrary host, 66th Society of Exploration Geophysicists Annual Meeting, Extended Abstracts, 978-981, Tulsa OK.

[10] Smith T., Conservative modeling of 3D electromagnetic fields; Part I: Properties and error analysis: Geophysics, 61, 1308-1318.

[11]Wannamaker P. E., Stodt J. A., and Rijo L., 1987, A stable finite element solution for two-dimensional magnetotelluric modeling: Geophysical Journal Royal Astronomical Society: 88, 277-296.